

slopes *always* come in multiples of -20dB/decade .

Fig. 1.41 shows the frequency response up to a fifth-order filter, where in each case all the resistors are the same value (R), and likewise the capacitors (C). The cut-off frequency for such an arrangement is still given by equation (1.47), but the total attenuation at this frequency increases by about -6.5dB for each extra filter section (not -3dB as might be expected, because each filter section loads the previous one and alters its behaviour*). The transfer functions for cascaded filters can again be derived using the principles of potential dividers, but it is much quicker to turn to circuit simulation for such designs.

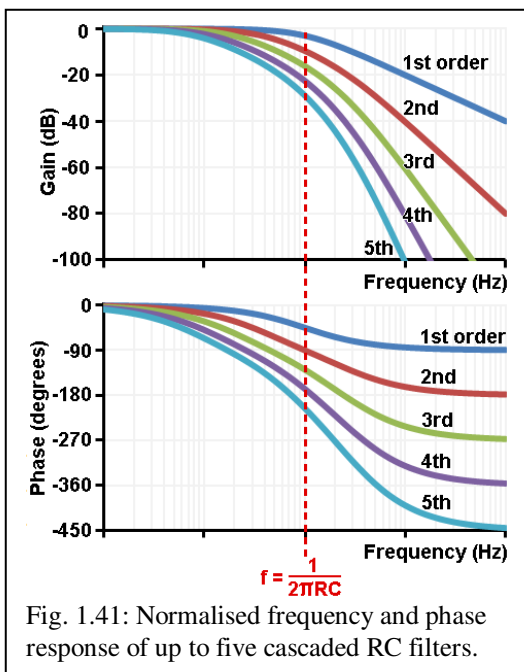


Fig. 1.41: Normalised frequency and phase response of up to five cascaded RC filters.

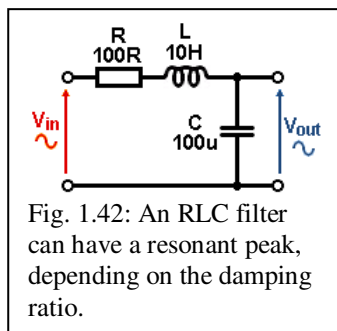


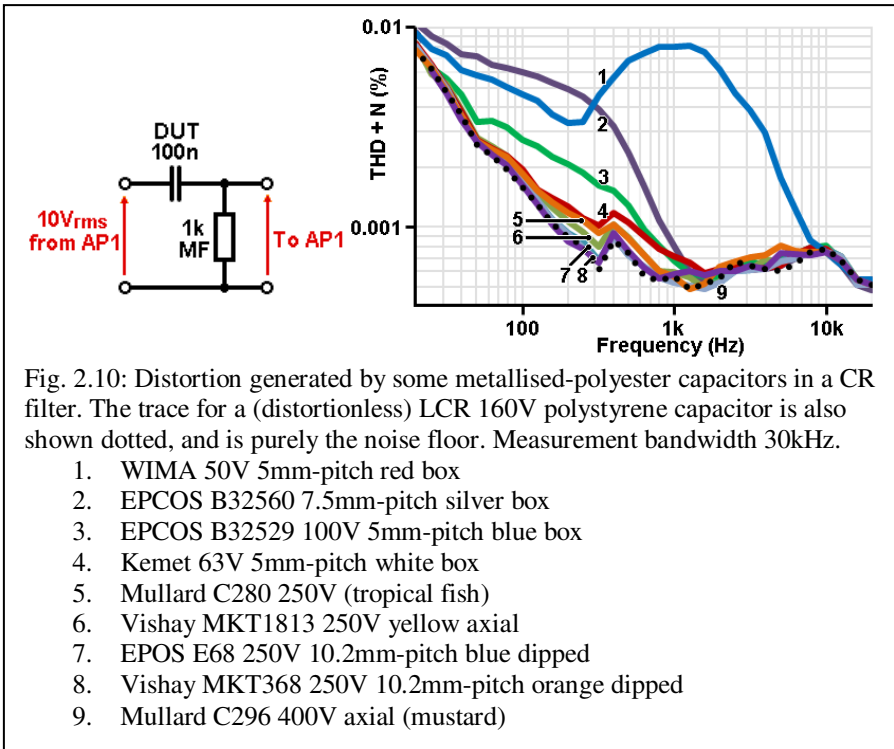
Fig. 1.42: An RLC filter can have a resonant peak, depending on the damping ratio.

Another type of second-order filter which is commonly encountered is an RLC filter, shown in fig. 1.42 (actually all we really need is L and C, but the resistance is an unavoidable part of a practical inductor and its effect on the circuit is worth knowing about). For variety, component values have been added which might represent a smoothing filter in a power supply. Having already encountered resonance in section 1.21 we should expect it to have some interesting effects on the frequency and phase response.

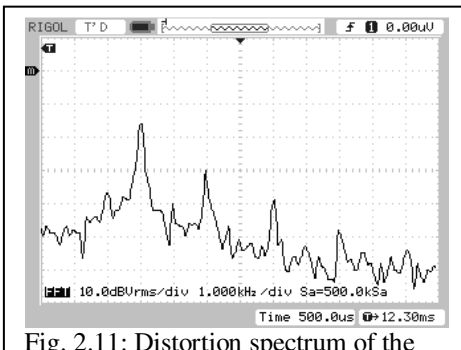
It will be remembered that the resistance in a resonant circuit controls the damping ratio, or Q, depending on what you're interested in. In this case the damping ratio is:

$$\zeta = \frac{R}{2} \sqrt{\frac{C}{L}} = \frac{R}{4\pi f_0 L} \quad (1.54)$$

* For this reason it is unwise to call a cut-off frequency a ‘ -3dB frequency’, because it is not always -3dB .



All of these are essentially distortionless and perfectly suitable for audio with the possible exception of polyester –the cheapest and most common type. There is much variation in the linearity of polyester capacitors, as demonstrated by fig. 2.10. Small-



volume box capacitors perform poorly, but at the same signal levels, higher-voltage physically-large devices show little or no measurable distortion. The devices which do produce distortion display a decaying series of odd harmonics. The worst performer in fig. 2.10 was a WIMA red box that apparently suffers from two sources of distortion: the first is the same as that exhibited by all capacitors while the second is proportional to the power flow in the device, producing the pronounced hump in the graph. Its spectrum is particularly rich (and variable), including some second harmonic, as shown in fig. 2.11. The way forward

Designing High-Fidelity Valve Preamps

transformers therefore increase the risks), and that the negative input resistance is proportional to g_m , so high- g_m valves are more likely to oscillate than low- g_m types. Good layout with short leads can reduce the possibility of oscillation, but is not a guaranteed cure. Reliably stopping oscillation requires the addition of a damping resistor to one or both offending areas, and such resistors are therefore called the **grid stopper** and **anode stopper**, as shown in fig. 3.42. The anode stopper may alternatively be placed in series with the output as in fig. 3.42b, in which case it may be called a **build-out resistor**.

The anode stopper must be small compared with r_a otherwise it will cause excessive increase of output resistance and undue loss of gain. Something between 10Ω and 100Ω is typical. Ideally, the positive resistance of the grid stopper cancels out any negative input resistance, and a value of about $2/g_m$ or 100Ω to $2k\Omega$ is generally sufficient. Larger values can be used for

more robust protection, although the added noise may be objectionable in sensitive applications like the front end of a phono stage. Also, do not forget that the grid stopper creates a low-pass filter with the Miller capacitance, so too much resistance could lead to loss of treble.

Stopper resistors must be mounted as close to the valve socket as possible in order to minimise lead inductance. Inductance in the cathode circuit is not usually a problem and may in fact stabilise an otherwise troublesome circuit. A cathode bypass capacitor naturally behaves like an inductor at the problem frequencies, though a ferrite ring around the cathode lead may also help. These precautionary components are very cheap insurance and a tell-tale sign of a knowledgeable circuit designer.

3.11: Slew Rate and Reactive Loads

The slew rate of an amplifier is the maximum rate at which the output voltage can change or 'slew' from one value to another. 'Speed' is sometimes used as a vague sort of synonym for slew rate, though it is not a technical term. The required slew rate depends on the highest frequency we want to amplify, and how much we need to amplify it, i.e. the voltage swing. This is important when driving

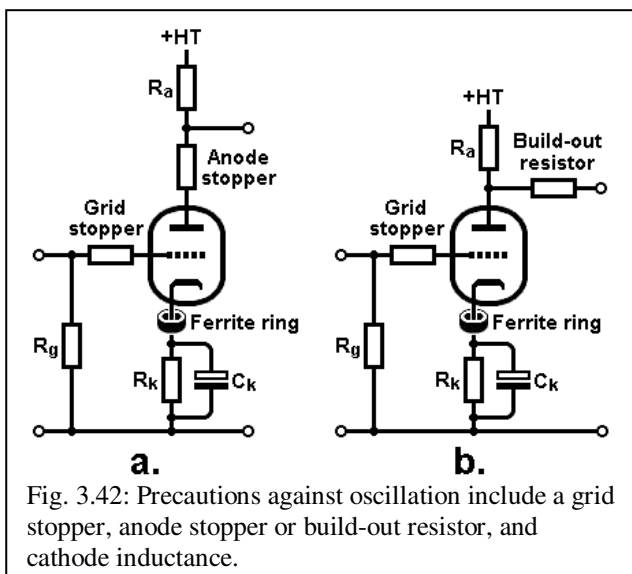
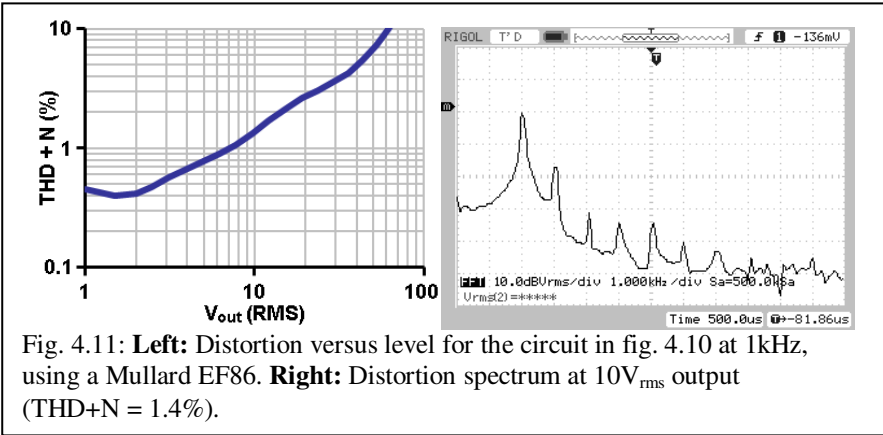
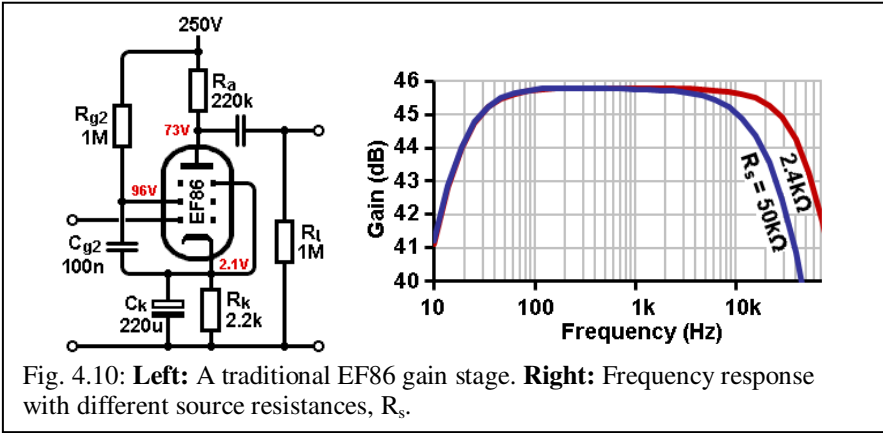


Fig. 3.42: Precautions against oscillation include a grid stopper, anode stopper or build-out resistor, and cathode inductance.



characteristic curve corresponding to the correct screen and bias voltage. This results in a predicted gain of about: $1\text{mA/V} \times 168\text{k}\Omega = 168$. The test circuit produced a figure of 195, suggesting g_m was closer to 1.16mA/V . Such high gain makes the valve prone to microphonics.

Fig. 4.10 also shows the frequency response of the circuit. The textbooks may boast about the wide bandwidth possible with pentodes, but this particular amplifier didn't get the message. The low-frequency end is limited to about 14Hz owing mainly to C_{g2}, while the high-frequency end is limited to 70kHz with a 2.4kΩ source resistance. Investigation showed to be due to an excessive output load capacitance of around 11pF (the measurement bandwidth was a reliable 130kHz and the circuit was built point-to-point on tag strip which should minimise wiring capacitance, so the author remains somewhat puzzled by this figure). Because the voltage gain is so high, even the slightest stray capacitance between grid and anode leads to significant Miller capacitance –about 110pF in this case. However, this is still much less than a high-gain triode would manage. Incidentally, leaving the internal electrostatic screen

Designing High-Fidelity Valve Preamps

model in fig. 5.11. These equivalent input noise voltages are simply the anode current noise densities divided by g_m^2 (squared because we are dealing with mean-square quantities):

$$V_{\text{EIN(shot)}}^2 = \frac{4k(0.644T_k)}{\sigma g_m} \quad \text{volts squared per hertz} \quad (5.18)$$

$$V_{\text{EIN(flicker)}}^2 = \frac{K}{g_m^2} \frac{I_a^2}{f} \quad \text{volts squared per hertz} \quad (5.19)$$

In fig. 5.12 these two equations are plotted for an average ECC83/12AX7 using values from table 5.4 and letting $T_k = 1000\text{K}$, $I_a = 1\text{mA}$, $g_m = 1.3\text{mA/V}$ (ignoring grid current noise for the time being). The point where the two types of noise are equal, i.e. the point where the two dashed lines cross, is the noise corner frequency. The total is the sum of the two noise sources, which can be added directly together since we're dealing with mean-square quantities. The basic shape of this plot is typical of all amplifying devices; only the relative levels of white and pink noise change, and with them the corner frequency. Fig. 5.13 compares the EIN densities of the triodes listed in table 5.4, all operating at the same anode current of 2mA.

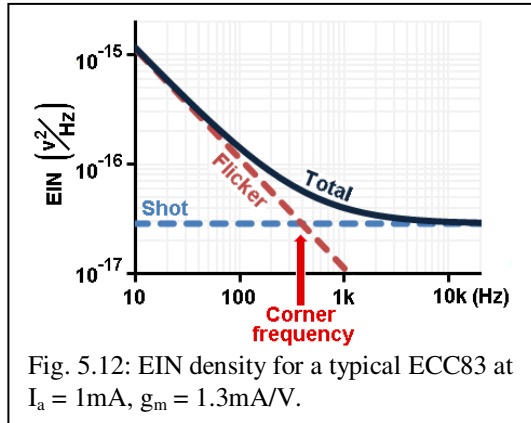


Fig. 5.12: EIN density for a typical ECC83 at $I_a = 1\text{mA}$, $g_m = 1.3\text{mA/V}$.

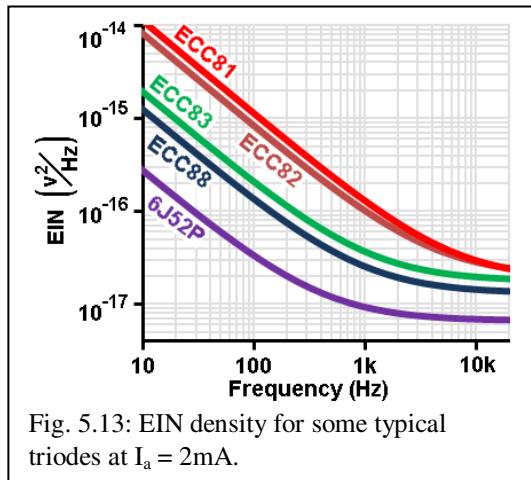


Fig. 5.13: EIN density for some typical triodes at $I_a = 2\text{mA}$.

Things get really interesting if we study equations (5.18) and (5.19) more closely. Notice that the shot noise power is inversely proportional to g_m , whereas the flicker noise power is proportional to I_a^2/g_m^2 . But g_m is approximately proportional to $\sqrt{I_a}$, so these two things are at odds; increasing anode current will *reduce* shot noise but *increase* flicker noise. The whole EIN spectral density does a kind of see-saw as anode current increases, as shown in fig. 5.14. Logically, therefore, the total noise in the audio band must reach a minimum at some intermediate, optimum value of anode current.

Fig. 6.35 shows some distortion results for resistive loading, which are also very similar to the ECC82. Under these conditions the third harmonic was barely visible at just over 30dB below the second, with all others lost in the noise floor.

6.2.6: 6Ж52П / 6J52P

Towards the end of the valve era a number of very-high- g_m frame-grid pentodes were developed to compete with transistors, and when operated as triodes they boast some of the lowest noise and best linearity of all valves. One such device is the Russian 6Ж52П / 6J52P ($\mu \approx 80$, r_a

$\approx 3k\Omega$). It is reportedly a cheap alternative to the European D3a which has recently become quite popular for phono preamps. However, these high- g_m valves rely on such tiny electrode spacings that they tend to be highly microphonic, have high grid current, and large interelectrode capacitances. Also, their construction is so critical that they often suffer a wider spread in parameters than 'ordinary' valves, so finding a matched pair may be tricky (and you only get one per bottle), so for these reasons their use in phono preamps may be counterproductive.

The author tested five specimens, connected as triodes (section 4.8). The valve has two cathode connections for low-inductance RF purposes, and the author initially made the mistake of joining the suppressor grid to one cathode pin while using the other cathode pin to connect to R_k/C_k . This resulted in excessive distortion at low output levels, which was cured by connecting both cathode pins together as in fig. 6.36.

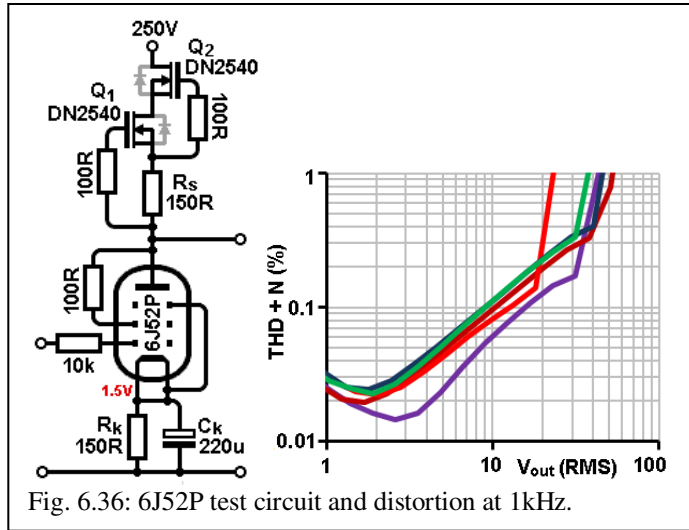


Fig. 6.36: 6J52P test circuit and distortion at 1kHz.

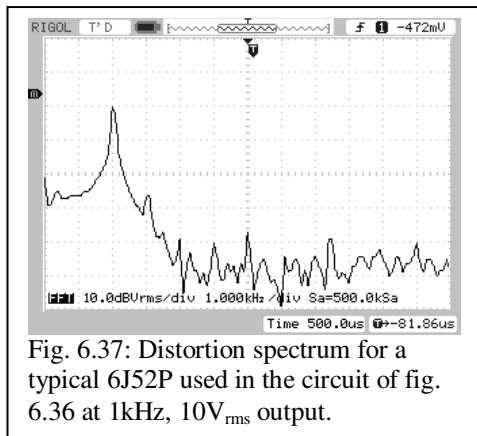


Fig. 6.37: Distortion spectrum for a typical 6J52P used in the circuit of fig. 6.36 at 1kHz, 10V_{rms} output.

This basic idea is illustrated in fig. 7.23. The first image shows a standard DC-coupled circuit with relative signal waveforms indicated. The signal is largest at the anode of V_1 and zero at the power supply, so the signal at the point half-way along the length of the anode resistor R_1 must be half the amplitude of the signal at the anode. The circuit in fig. 7.23b shows the bootstrap transformation.

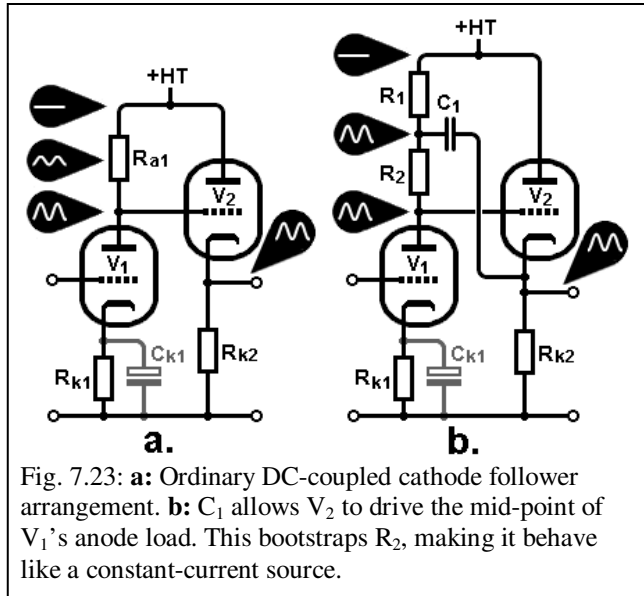


Fig. 7.23: **a:** Ordinary DC-coupled cathode follower arrangement. **b:** C_1 allows V_2 to drive the mid-point of V_1 's anode load. This bootstraps R_2 , making it behave like a constant-current source.

R_1 has been split into two parts and the output of the cathode follower is coupled to the junction via C_1 . If C_1 is large and the cathode follower is perfect and has unity gain, then the signal at the anode of V_1 is fed to the cathode follower and is immediately buffered and passed back to the junction of R_1 - R_2 , so exactly the same signal voltage appears at both ends of R_2 . With no difference in AC voltage across this resistor, there can be no AC current in it, so it would appear to have infinite resistance. Another way of looking at it is to say that if C_1 is large then as far as AC signals are concerned R_2 appears to be connected directly between grid and cathode of V_2 , hence it is bootstrapped and behaves like a constant-current source load for V_1 . The gain of V_1 will then be equal to its μ ,

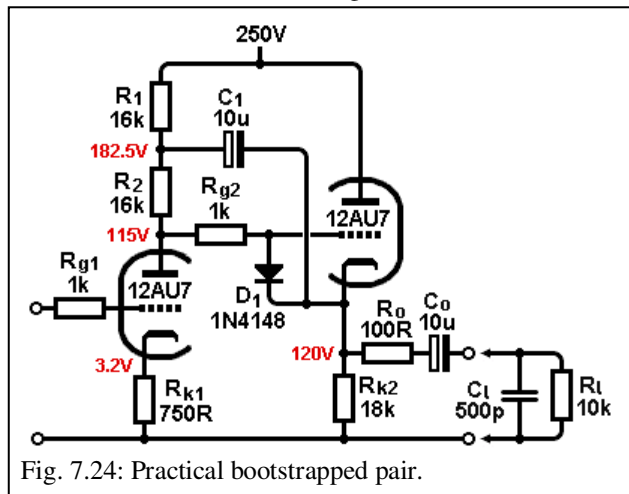
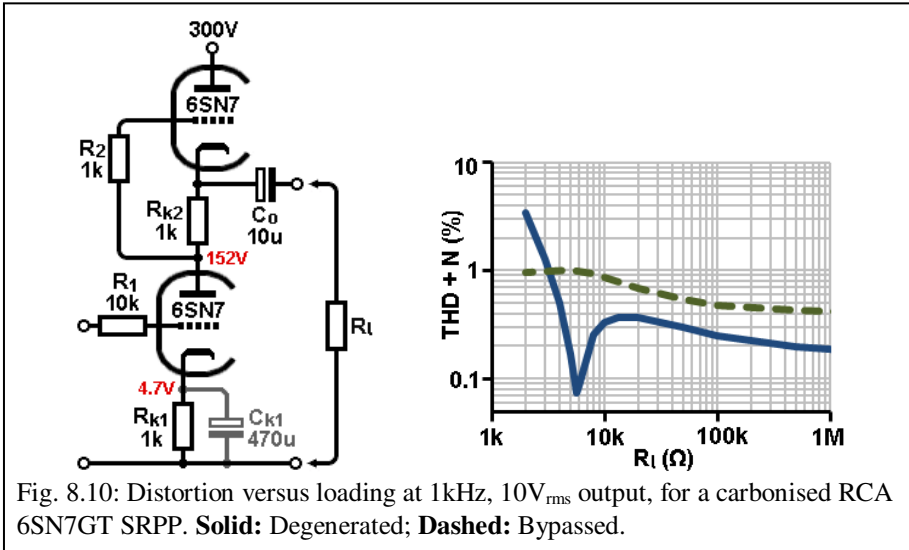


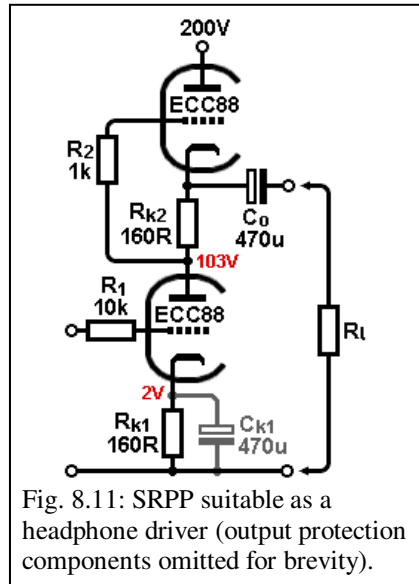
Fig. 7.24: Practical bootstrapped pair.

¹¹ Bennett, R. (2006). An Improved Split-Load Phase Inverter, Audio Xpress, July, pp25-7.

¹² Blencowe, M. (2012). *Designing Valve Preamps for Guitar and Bass*. Lulu, pp129-32.



Since the SRPP shares so much in common with the White cathode follower it too is sometimes used to drive heavy loads such as headphones. To complete this section then, fig. 8.11 shows an ECC88 headphone driver biased to the same quiescent current as the White cathode follower example from section 7.14.3. In practice, a build-out LR network and protection Zeners should be added, but they are omitted here for brevity. Fig. 8.12 shows distortion versus output power for both the degenerated and bypassed case. The optimum load predicted by equation (8.9) is about 750Ω, while the experimental value was 1.2kΩ for the degenerated case. This circuit is therefore not strictly optimised for typical headphone impedances as R_{k2} is too large. Nevertheless, it does manage to deliver enough output power for the job, but the distortion is about an order of magnitude worse than for the White cathode follower. Interestingly, the bypassed SRPP produces less distortion with heavy loads than the degenerated case, although its behaviour is more complex.



The degenerated output impedance was 1.5kΩ and the unloaded gain was 15.3, while for the bypassed case the figures were 810Ω and 23 respectively. Since both the distortion and output impedance are much too high for direct use with

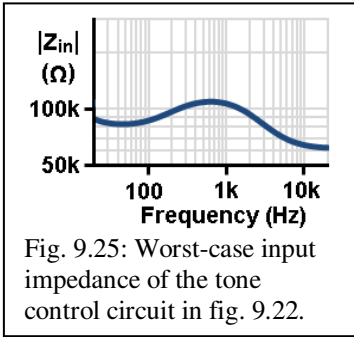


Fig. 9.25: Worst-case input impedance of the tone control circuit in fig. 9.22.

setting the gain was exceptionally flat at $-0.7\text{dB} \pm 0.1\text{dB}$ between 18Hz and 40kHz. The coverage is also attractively symmetrical, and the cut/boost is more even (in decibels) with pot rotation than the passive control from section 9.4.1. Fig. 9.24 shows distortion versus frequency for a constant *input* level of $10V_{\text{rms}}$. At full boost there is less feedback and a larger output level, so distortion increases, and *vice versa*. But even at full boost the figures are quite low, considering the signal level, and in a typical

hi-fi system the circuit would probably be handling much smaller input levels so the distortion would be proportionately lower during actual use. The worst-case input impedance occurs with both controls at full boost and is plotted in fig. 9.25 (simulated), falling to a minimum of 62k Ω .

9.4.4: Active Tilt Control

The passive tilt control from section 9.4.2 can also be placed in a feedback loop, and exactly the same design principles apply as discussed in the previous section. If the source resistance cannot be kept below of couple of kilohms then an equal resistance should be added in the feedback path. Provided R_g is relatively large then it is bootstrapped to the point

where a balancing resistance between input and grid is not required to maintain flatness.

Maximum bass boost is equal to $(R_4+P_1)/R_1$, and equal boost and cut obtain using the same equation as for the passive circuit. The worst-case input impedance occurs at maximum treble boost and is a little more than half R_3 , so it is desirable to make this larger than 100k Ω . Since this also determines R_2 , and assuming we already have a potentiometer in mind, we can then find R_1 .

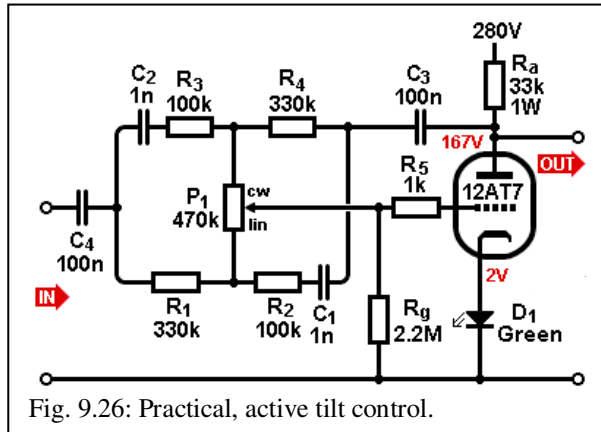


Fig. 9.26: Practical, active tilt control.

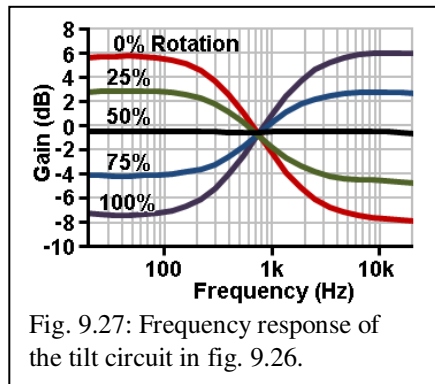


Fig. 9.27: Frequency response of the tilt circuit in fig. 9.26.

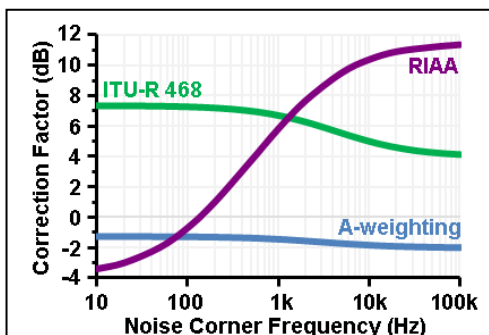


Fig. 10.14: Correction factors for converting unweighted 20Hz–20kHz noise into weighted noise in the presence of pink noise, assuming RMS metering. Reproduced from fig. 5.9.

don't want to add much more to this. A final, unweighted SNR of 70dB relative to 5mV can be considered a good effort for a pure-valve phono preamp.*

Recall that RIAA equalisation greatly worsens the noise figure if there is much pink-noise content, as shown by fig. 10.14. The input valve therefore needs to be one with both low shot noise *and* low flicker noise. Unfortunately, these are conflicting requirements, because shot noise is reduced by maximising g_m (and therefore I_a), whereas flicker noise is reduced by

minimising I_a . This implies using a high- g_m device at only a moderate anode current; 2 to 3mA is usually the best compromise. The need for very low noise and microphonics immediately rules out most pentodes unless they are triode-connected. Normally we would also consider using several devices in parallel to reduce the EIN, but this is not always possible with triodes because it multiplies the already-high Miller capacitance.

Fig. 10.15 shows the equivalent input noise voltage spectral density of some triodes. The ECC81/12AT7 and ECC82/12AU7 are clearly the noisiest, mustering an EIN rarely better than $1\mu\text{V}$ in the audio band, which is about as high as we should dare to go. The 6J52P/6Ж52П (triode connected) appears the best, but the hidden variables are that such high- g_m pentodes suffer acutely from microphonics and parameter spread, so will need to be hand-selected, and they invariably have unworkably high Miller capacitance too. The ECC88/6DJ8 is a popular choice as it can achieve an EIN of about $0.6\mu\text{V}$ on a good day, with Miller capacitance around 100pF, though it too suffers noticeably from microphonics. The ECC83/12AX7 is a

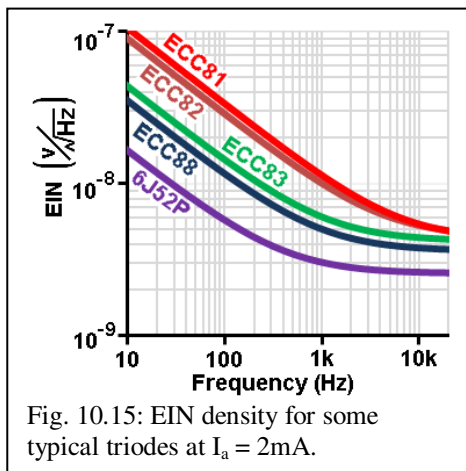


Fig. 10.15: EIN density for some typical triodes at $I_a = 2\text{mA}$.

* Be aware that many commercial manufacturers use weighted or invalid measurement techniques to boost their advertised figures.

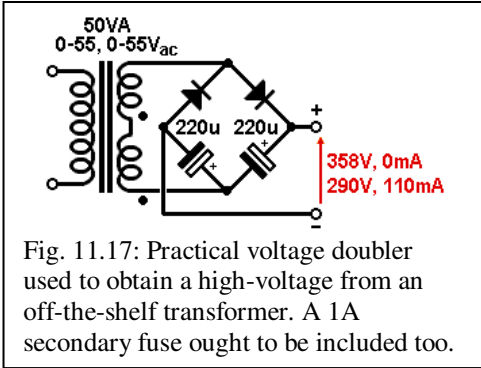


Fig. 11.17: Practical voltage doubler used to obtain a high-voltage from an off-the-shelf transformer. A 1A secondary fuse ought to be included too.

Notice that the maximum load power is 32W but a 50VA transformer is required, i.e. the power factor is 0.64, which is no different from an ordinary full-wave power supply. The diodes must be rated for $>380V_{\text{r.m.s}}$ and $>220\text{mA}$. The 1N4004 is rated for $400V_{\text{r.m.s}}$ and 1A, but the ubiquitous 1N4007 could of course be used too. Not only is this technique convenient because it uses an off-the-shelf transformer, but the capacitors need

only be 200V rated, and we have the freedom to use a separate heater transformer of any desired voltage. All of this may be easier to obtain and perhaps cheaper than a traditional design using a dedicated valve transformer.

Another common application of the voltage doubler uses the junction of the two capacitors as the ground reference, thereby creating a bipolar supply (the ripple on each rail will then be at mains frequency even though it is a full-wave circuit as far as the transformer is concerned). This approach is often useful for equipment supplied by an external AC voltage adapter (US: wall wart). Fig. 11.18 shows a typical example using a 12V, 12VA transformer, and note that

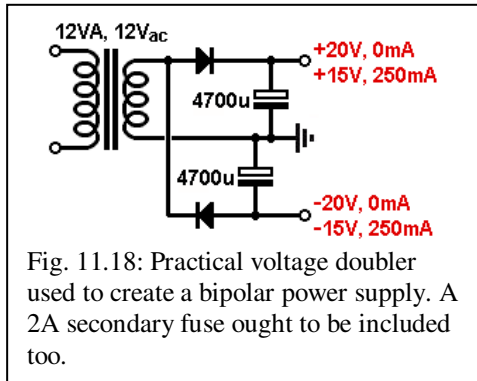


Fig. 11.18: Practical voltage doubler used to create a bipolar power supply. A 2A secondary fuse ought to be included too.

there is a fair amount of sag between no-load and full-load conditions, owing to the poor regulation of such a small transformer. The two supply rails should be equally loaded to avoid a net DC current in the transformer (core saturation). The diodes

must be rated for $>40V_{\text{r.m.s}}$ and $>500\text{mA}$, so 1N4001s could be used ($50V_{\text{r.m.s}}$, 1A).

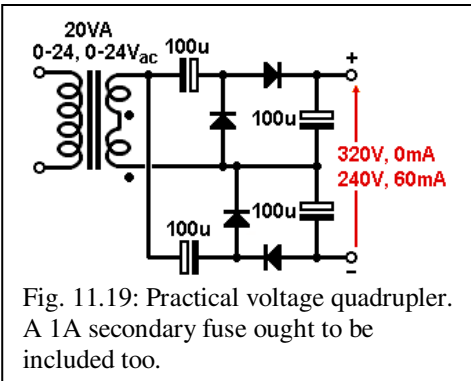


Fig. 11.19: Practical voltage quadrupler. A 1A secondary fuse ought to be included too.

Transformer voltages can be multiplied by more than two times with more extensive rectifier circuits, but at the expense of ever declining load regulation and power factor. Fig. 11.18 shows an example of a voltage quadrupler using a cheap 20VA, 0-24, 0-24V_{ac} transformer from which 240V_{dc} is obtained at 60mA